[42]

A. DI GERLANDO, S. FORTUNA, I. VISTOLI

ARMATURE CURRENT UNBALANCE DETECTION USING ON-BOARD PROBE WINDINGS FOR THE STATOR ON-LINE DIAGNOSTICS OF EMS MAGLEV SYSTEMS

14th INTERNATIONAL CONFERENCE ON MAGNETICALLY LEVITATED SYSTEMS
(MAGLEV '95)
BREMA, GERMANIA
27-29 NOVEMBRE 1995

MAGLEV '95

14th International Conference on Magnetically Levitated Systems

November 26 – 29, 1995
Hotel Maritim Bremen, Germany

Scientific Chairman

Prof. Dr.-Ing. Dr. h. c. Herbert Weh	TU Braunschweig Institut für Elektrische Maschinen, Antriebe und Bahnen

Technical Committee

Prof. Tony Eastham	Queen's University, Dept. of Electrical Engineering, Kingston, Canada
Prof. Dr. Eisuke Masada	The University of Tokyo, Dept. of Elekctrical Engineering, Tokyo, Japan
Prof. Augusto Morini	University of Padova, Dept. of Electrical Engineering, Padova, Italy
Dr. Donald M. Rote	Agronne National Laboratory, Center for Transportation Research, Argonne II, USA

Organizing Committee

Dipl.-Ing D. Rogg	Dornier System Consult, Friedrichshafen
Dipl.-Ing. Willi J. Mayer	Dornier System Consult, Friedrichshafen

Organized by

VDE Association of German Electrical Engineers and Power Engineering Society (ETG) within VDE, Sponsored and Co-sponsored by EUREL, Dornier, Dyckerhoff & Widmann and others

VDE-VERLAG GMBH · Berlin · Offenbach

Armature Current Unbalance Detection using On-board Probe Windings for the Stator On-line Diagnostics of EMS Maglev Systems

Di Gerlando, Antonino Fortuna, Stella Vistoli, Ivo
Dipartimento di Elettrotecnica - Politecnico di Milano, Milano, Italy

Abstract - The continuity and the reliability of the service in the Maglev systems are fundamental features. On-line diagnostics devices, suited to timely detect possible conditions of incoming faults, are very important issues.
The possibility to locate anomalous operating conditions in stator sectors of EMS Maglev systems by measurements of the armature current unbalance (via electromagnetic induction) is analysed.
To this aim, suited probe windings, disposed in the field poles of the vehicle, are used: the operation modes of these windings are analysed, together with their design criteria and their compatibility with the basic features of the system.
The possibility of detecting anomalous operating conditions in the stator guide windings and in the supply devices is discussed. The method, based on the measurement of the stator current unbalance, makes use of suited probe windings located into the on-board part of the linear synchronous motor (LSM); the operating mode of these probe windings and their problems of compatibility with the Maglev system characteristics are analysed.
In their simplest version, these probe windings can be built up with single coils, equipped with very small cross-section wires, located towards the air-gap in a pair of slots cut into the excitation-levitation system saliency, along both sides of the vehicle.
Extra m.m.f. harmonic fields are generated in the air-gap under unbalanced stator currents operating conditions: these fields induce extra e.m.f. harmonic components in the probe turns, that can be used as an index of the stator current unbalance.
The considerations that make the proposed measurement method better than pure three-phase current measurements performed in the substations (surely more direct and simple) are the following:
- during the LSM steady-state operation, the current controlled PWM inverters of the substations are regulated in such a way to feed the phase windings of the active armature sections with balanced currents; thus, if these inverters operate correctly, actually they deliver three balanced currents; in these conditions, the measurements in the substations can only confirm the balanced operation of the inverters, but do not allow any direct check about the currents flowing in the guide windings;
- in case of degradation of the armature windings insulation, a local (even small) unbalance of the phase currents can occur, without any possibility of detection of this anomalous situation by the substation monitoring system; nevertheless, this unbalance is an important index of a beginning damage that, if not detected and removed, can cause more serious faults;
- an on-board diagnostics system of measurement and computation, using a probe winding for the detection of the magnetic effects of local unbalance, allows the real-time fault monitoring in every winding section, quickly informing the ground surveillance system about the position of the abnormal portion and about the amount of the unbalance.

1. Introduction

A factor of strategic importance in the realisation and management of Maglev transportation systems is given by the availability of devices for the on-line diagnostics, which minimise the risk of unexpected faults, limiting the maintenance costs and ensuring safety and reliability during normal operation: these objectives have utmost importance, also for the need to make Maglev systems competitive compared with the other high speed conventional systems.
Thus, an automatic system for the preventive maintenance is necessary, in order to accomplish a real-time monitoring, based on the data collected during the vehicle motion, processed on board and transmitted to the receivers disposed in the supply substations.
Certainly, a great deal of interest has been devoted to this subject by many researchers, despite of the lack of complete informations in the specialised literature, maybe because of industry security reasons.
In fact, the diagnostics problems in Maglev systems are wide and various, also because of the complexity and of the different kind of their components; therefore, in this paper the attention is devoted to analyse some methodological aspects about the diagnostics of electrical components of the stator guide: indeed, the stator guide is a very important subsystem, since it is distributed all along the line and therefore particularly exposed to the risk of faults.

Work supported by the Italian Research National Council (CNR).

In the paper the following aspects about the operation and the design of the probe winding are analysed:
- decomposition of the unbalanced currents into terns of symmetrical components, with evaluation of harmonic order and amplitudes of the e.m.f.s induced by the corresponding m.m.f. harmonic fields;
- choice of the harmonic e.m.f. which is more suited to give an index of the stator current unbalance;
- analysis of the e.m.f. induced in each probe turn as a function of the coil pitch and choice of its optimal value;
- evaluation of the dependence of the probe winding signal on the LSM toothed structure and on the presence of the linear synchronous generator.

2. General notes and hypotheses

The analysis is based on the following hypotheses:
- the linear synchronous motor here considered is characterised by a three-phase armature winding with q=1 slots/(pole·phase) and by a salient pole field structure with concentrated excitation windings (see Fig.1): the most important parameter of the LSM is the pole pitch τ_s, linked to the vehicle speed (v_s) and to the frequency of the inverter feeding the LSM (f_s) by the well known expression:

$$v_s = 2 \cdot f_s \cdot \tau_s \; ; \qquad (1)$$

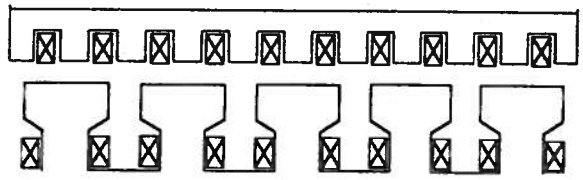

Fig.1 Schematic structure of the active portion of a EMS Maglev system, with armature winding consisting of 1 slot/(pole·phase) and with excitation-levitation salient poles disposed on board.

- the LSM three-phase armature winding is interested by a tern of sinusoidal currents: this hypothesis is justified by assuming that the converters are PWM current controlled inverters;
- the LSM is considered operating in steady-state conditions: in fact, transient conditions with instantaneous current unbalance could be wrongly interpreted as fault conditions: thus, the detecting system must be excluded during starts and stops;
- the magnetic voltage drops in the iron branches are considered zero: this is acceptable, because the flux density in ferromagnetic circuit is low, for reasons of control and of levitation safety: thus, there is a linear link between fluxes and m.m.f.s;
- it is assumed that the air gap m.m.f. can be decomposed in terms of Fourier series: this corresponds to neglect the end effects, that is acceptable thanks to the great number of poles existent on the vehicle;
- at the beginning, the influence of the tooth-slot permeance fluctuations during motion is neglected;
- moreover, in the preliminary analysis, the effect of the loaded operation of linear on-board synchronous generators is neglected.

The level of acceptability of the last two hypotheses will be discussed ahead.

3. The harmonic m.m.f. fields

3.1. Harmonic m.m.f. fields in the normal operation

With the adopted hypotheses (q=1), the winding factor of the LSM windings equals unity; moreover, being unity the number of stator conductors in the slot (u=1), it follows that in each section the total number of conductors equals its number of poles.
During the operation with balanced currents, some harmonic m.m.f. fields are generated in the air gap; all of them are tooth harmonic fields, with order:

$$h = 1 + 6 \cdot k \; ; \quad k = 0, \pm 1, \pm 2, \ldots \; ; \qquad (2)$$

the amplitude of these m.m.f.s equals:

$$M_{M_h} = \frac{3 \cdot \sqrt{2}}{\pi} \cdot \frac{I}{|h|} \; , \qquad (3)$$

where I is the stator phase current.
The speed (v_{s_h}) of the generic harmonic field with order h, referred to a stator fixed frame, is given by:

$$v_{s_h} = v_s / h = 2 \cdot f_s \cdot \tau_s / h = 2 \cdot f_s \cdot \tau_{s_h} \; , \qquad (4)$$

where v_s is the synchronous speed, which is equal to the main field one, measured referred to the stator.
The fields with order h = +7, +13, +19, ... travel in the running way of the fundamental field, while the fields with order h = −5, −11, −17, ... travel in the opposite running way of the fundamental field.
Called v_h the speed of the h^{th} harmonic field, measured with reference to the vehicle in motion, we have:

$$v_h = v_{s_h} - v_s = v_s \cdot (1 - h)/h \; . \qquad (5)$$

A generic active conductor disposed at the air gap on the surface of the vehicle field poles sees the variation of the harmonic fields with frequency:

$$f_h = \left| \frac{v_h}{2 \cdot \tau_{s_h}} \right| = \left| \frac{v_s \cdot (1-h)}{2 \cdot h} \cdot \frac{h}{\tau_s} \right| = f_s \cdot |6 \cdot k| \; . \qquad (6)$$

Thus, this conductor sees the stator harmonic m.m.f.s two by two with the same frequency, multiple of a factor $|1-h|$ of the LSM feeding frequency: therefore, the 5^{th} and 7^{th} order fields generate an e.m.f. with frequency $6 \cdot f_s$, the 11^{th} and 13^{th} order fields induce an e.m.f. of frequency $12 \cdot f_s$ and so on [1].
The above written is valid if the stator currents constitute a balanced three-phase system: in this case there is a translating field with just one fundamental harmonic, synchronous in the same running way of the vehicle.

3.2 Additional harmonic m.m.f. fields due to the stator current unbalance

If the three stator currents are unbalanced, it is possible to decompose them into symmetrical terns, that is homopolar, direct and inverse terns.
The presence or not of the homopolar tern depends on the system configuration and on the kind of fault: in any case, considering that these homopolar current components produce at the air gap a m.m.f. field that is identically zero, their presence is not relevant for the evaluation of the unbalance.
Thus, the analysis will be limited just to the direct and inverse terns: as known, these terns have current phasors with opposite cyclic sense, and therefore the corresponding fundamental m.m.f. running fields travel in opposite ways in the air gap.

As known, each of the terns produces harmonic m.m.f.s with order $h = 1 + 6\cdot k$.
If we consider positive the running way of the vehicle (in accordance with that of the fundamental field of the direct tern), in case of inverse tern the fields with order h = +7, +13, +19, ... travel in the opposite way of the fundamental field; vice versa, the fields with order h = −5, −11, −17, ... travel in the same way of the fundamental field.
The speed of the h^{th} harmonic m.m.f. produced by the inverse tern, with respect to the vehicle, equals:

$$v_h = -v_s/h - v_s = -v_s\cdot(1+h)/h \quad . \qquad (7)$$

In this case, the frequency of the e.m.f.s induced in an active conductor on-board of the vehicle equals:

$$f_h = \left|\frac{v_h}{2\cdot\tau_{s_h}}\right| = \left|\frac{v_s\cdot(1+h)}{2\cdot h}\cdot\frac{h}{\tau_s}\right| = f_s\cdot|2+6\cdot k| . \qquad (8)$$

Thus, with different values of k, the following frequency harmonic orders will be induced:

$$\begin{aligned} f_h/f_s &= 2, 8, 14, \ldots \text{ for } k = 0, +1, +2, \ldots \\ f_h/f_s &= 4, 10, 16, \ldots \text{ for } k = -1, -2, -3, \ldots \end{aligned} \quad . \qquad (9)$$

Eq.(9) points out two important differences compared with the frequencies given by eq.(6):
- the inverse tern fundamental field produces a double frequency e.m.f., while the direct tern fundamental field, synchronous with the vehicle, does not produce any e.m.f.;
- differently from what happens for the direct tern, the couple of values ±k does not produce two e.m.f.s with the same frequency.

4. The on-board harmonic e.m.f.s

The rms value of the harmonic e.m.f. e_h in each active conductor with length ℓ_e (transversal width of the lamination stack of each stator guide side) equals:

$$e_h = \left(B_{M_h}/\sqrt{2}\right)\cdot\ell_e\cdot v_h \qquad (10)$$

where the maximum flux density B_{M_h} is given by:

$$B_{M_h} = \mu_o\cdot\frac{M_{M_h}}{\delta} = \frac{3\cdot\sqrt{2}}{\pi}\cdot\frac{\mu_o}{\delta}\cdot\frac{I}{|h|} ; \qquad (11)$$

δ is the width of the LSM air gap.
Thus, eq.(10) becomes:

$$e_h = \left(\frac{6\cdot\mu_o}{\pi}\cdot\frac{\tau_s\cdot\ell_e}{\delta}\right)\cdot I\cdot\frac{f_h}{h^2} = K_e\cdot I\cdot\frac{f_h}{h^2} ; \qquad (12)$$

in eq.(12) the term within brackets, indicated with K_e, can be considered constant for a given system.
By distinguishing in eq.(12) the harmonic e.m.f.s due to the direct (I_d) and inverse (I_i) tern, we have:

$$\begin{aligned} e_{d_h} &= K_e\cdot I_d\cdot f_s\cdot 6\cdot|k|/(1+6\cdot k)^2 \\ e_{i_h} &= K_e\cdot I_i\cdot f_s\cdot|2+6\cdot k|/(1+6\cdot k)^2 \end{aligned} \quad . \qquad (13)$$

The induced e.m.f.s e_{d_h} and e_{i_h} are linearly linked to the feeding frequency and therefore to the vehicle speed and to the amplitude of the current phasors of the direct and inverse terns.
It is useful to define the following e.m.f. coefficients:

$$\alpha_d(k) = \frac{6\cdot|k|}{(1+6\cdot k)^2} ; \quad \alpha_i(k) = \frac{|2+6\cdot k|}{(1+6\cdot k)^2} . \qquad (14)$$

They are not dimensionally e.m.f.s, but their evaluation allows a comparison among the amplitudes of the harmonic e.m.f.s that each tern induces on the basis of eq.(13); the corresponding values for the lowest harmonic orders are given in Tables I and II.

Table I - Frequencies and e.m.f. coefficients induced by the direct tern of the stator currents.

k	h	f_h/f_s	$\alpha_d(k)$
0	+1	0	0.000
−1	−5	6	0.240
+1	+7	6	0.122
−2	−11	12	0.099
+2	+13	12	0.071
−3	−17	18	0.062
+3	+19	18	0.050

Table II - Frequencies and e.m.f. coefficients induced by the inverse tern of the stator currents.

k	h	f_h/f_s	$\alpha_i(k)$
0	+1	2	2.000
−1	−5	4	0.160
+1	+7	8	0.163
−2	−11	10	0.083
+2	+13	14	0.083
−3	−17	16	0.055
+3	+19	20	0.055

The most important e.m.f.s of the direct tern are those having both frequency six times the fundamental, induced by the m.m.f.s of order 5^{th} and 7^{th}; the

wider effect is due to the harmonic m.m.f.s running in the opposite way with respect to the vehicle.
For the inverse tern, the induced 2nd harmonic e.m.f. amplitude is greater than the other e.m.f.s; moreover, while the $\alpha_i(k)$ values are roughly symmetrical with respect to $|k|$, the values of f_h/f_s are not symmetrical.

By assuming, as reference value, the LSM rated current, the following quantities

$$\dot{I}_d = I_d/I_n \qquad \dot{I}_i = I_i/I_n \tag{15}$$

are the p.u. values of the direct and inverse current respectively, referred to the LSM rated current.
On the other hand, for the 2nd of (15) we can write:

$$\dot{I}_i = \frac{I_i}{I_d}\cdot\dot{I}_d = \rho_I\cdot\dot{I}_d \quad , \tag{16}$$

where ρ_I is the current unbalance factor.
In (15) and (16) $\dot{I}_d$ represents, in p.u., the load condition of the LSM, while $\dot{I}_i$, proportional to ρ_I, is the index of the anomalous operation of the stator.
If we consider a value of direct current I_d equal to the rated one I_n (that is $\dot{I}_d = 1$), the p.u. values of the inverse current ($\dot{I}_i$) coincide with the values of the current unbalance factor $\rho_I = I_i/I_d$.

Only a detailed analysis of the operating conditions of the system (that links the type and the level of the anomalous operation with the current unbalance factor) can allow to establish which is the minimum value of the unbalance for which a fault of the stator guide can be considered imminent: the present analysis will be limited to consider the link between the unbalance level and the diagnostic signal obtainable by the probe winding.
To this aim, by noting with $\dot{e}_{d_h}(k)$ and $\dot{e}_{i_h}(k)$ the following non-dimensional quantities:

$$\dot{e}_{d_h}(k) = \alpha_d(k)\cdot\dot{I}_d \;;\; \dot{e}_{i_h}(k) = \alpha_i(k)\cdot\dot{I}_i \tag{17}$$

the real values of the harmonic e.m.f.s are:

$$\begin{aligned} e_{d_h}(k) &= \dot{e}_{d_h}(k)\cdot K_e\cdot f_s\cdot I_n \\ e_{i_h}(k) &= \dot{e}_{i_h}(k)\cdot K_e\cdot f_s\cdot I_n \end{aligned} \tag{18}$$

Considering that the proportionality factor $K_e\cdot f_s\cdot I_n$ is common to both the equations of (18), the comparison among the harmonic e.m.f.s of the direct and inverse terns can be performed by means of the corresponding e.m.f.s expressed in p.u., ignoring the values of the LSM rated current and frequency f_s.

4.1. The harmonic e.m.f. components induced in the probe winding

The amplitudes of the harmonic e.m.f.s induced in the probe winding are evaluated in the following.
The h^{th} harmonic e.m.f. equals:

$$E_h = 2\cdot N_t\cdot e_h\cdot k_{w_h} \;; \tag{19}$$

in eq.(19) N_t is the number of turns of the probe winding; k_{w_h} is the winding factor of the h^{th} harmonic, equal, in general, to the product between the distribution factor (here equal to unity, because q=1) and the pitch factor. In this case we have:

$$k_{w_h} = \sin\left(\frac{\gamma_h}{2}\right) = \sin\left(\frac{\pi}{2}\cdot\frac{\tau}{\tau_{s_h}}\right) = \sin\left(\frac{\pi\cdot\tau\cdot h}{2\cdot\tau_s}\right), \tag{20}$$

where γ_h is the displacement angle between the phasors of the e.m.f.s induced in the active sides of the probe winding and τ is its pitch.
Let indicate with

$$\dot{\tau} = \tau/\tau_s \tag{21}$$

the pitch of the probe winding, expressed in p.u. referred to the pole pitch τ_s of the LSM.
The harmonic e.m.f.s induced in the probe winding by the harmonic m.m.f. fields (fields whose amplitudes are proportional to the currents of the direct and inverse terns) have amplitude depending on the pitch $\dot{\tau}$; from the previous relations we obtain:

$$\begin{aligned} E_i(k,\dot{I}_i,\dot{\tau}) &= 2\cdot N_t\cdot e_{i_h}\cdot\left|\sin\left(\pi\cdot\dot{\tau}\cdot|1+6\cdot k|/2\right)\right| \\ E_d(k,\dot{I}_d,\dot{\tau}) &= 2\cdot N_t\cdot e_{d_h}\cdot\left|\sin\left(\pi\cdot\dot{\tau}\cdot|1+6\cdot k|/2\right)\right| \end{aligned} \tag{22}$$

The observation of (20) and (22) suggests that:
- the harmonic e.m.f.s generated by the two terns become zero for values of the probe winding pitch τ equal to multiple even of the pole pitch $\tau_{s_h} = \tau_s/h$ of the inducing harmonic m.m.f.;
- the harmonic e.m.f.s generated by the two terns become maximum for values of the probe winding pitch τ equal to multiple odd of the pole pitch $\tau_{s_h} = \tau_s/h$ of the inducing harmonic m.m.f..

4.2. Analysis of the probe winding e.m.f.s as a function of the pitch

Fig.2 shows the amplitude diagram of the harmonic e.m.f.s $E_i(k,\dot{I}_i,\dot{\tau})$ generated by the inverse current tern for k equal to 0, −1, +1 (corresponding to the fields with order 1, 5, 7 respectively), as a function of the pitch $\dot{\tau}$: as already shown, these e.m.f.s have order 2, 4, 8 respectively, referred to the LSM frequency; the diagrams are drawn for $\dot{I}_i = 0.1$ and the e.m.f.s are in p.u., referred to the quantity $N_t\cdot K_e\cdot f_s\cdot I_n$.
Fig.3 shows the amplitude diagrams of the harmonic e.m.f.s $E_d(k,\dot{I}_d,\dot{\tau})$ induced by the direct current tern, as a function of $\dot{\tau}$; the e.m.f.s (again expressed in p.u., referred to $N_t\cdot K_e\cdot f_s\cdot I_n$) are drawn for k equal to −1 and +1 (harmonic fields with order 5 and 7, whose e.m.f.s have frequency $6\cdot f_s$), with $I_d = I_n$.
Of course, in Fig.s 2 and 3 the extension of the pole pitch $\dot{\tau}$ in the range 0-1 is merely theoretical: in fact, the obtainable values belong to the central zone only.
Fig.s 2 and 3 suggest what follows:
- for the curves obtained with k= +1 (e.m.f.s generated by the m.m.f. field with order h= +7) we have:
  - the e.m.f. with frequency $8\cdot f_s$, generated by the inverse tern, becomes zero for the same values

of $\dot{\tau}$ for which the e.m.f. with frequency $6 \cdot f_s$, induced by the direct tern, becomes zero;
- these harmonic e.m.f.s become zero for values of τ equal to multiple even of $\tau_s/7$;
- the induced e.m.f.s show maximum values for values of τ equal to multiple odd of $\tau_s/7$.

– similar remarks can be made as regards the zero crossings and the maximum values of the harmonic e.m.f.s corresponding to k= −1, generated by the m.m.f. field with order h= −5;
– for k=0 (fundamental m.m.f. field: h= +1) the double frequency harmonic e.m.f., induced by the inverse tern, always shows values different from zero and increasing with the growth of τ: this happens because the inducing field has a pitch equal to the LSM pitch and τ is always lower than it.

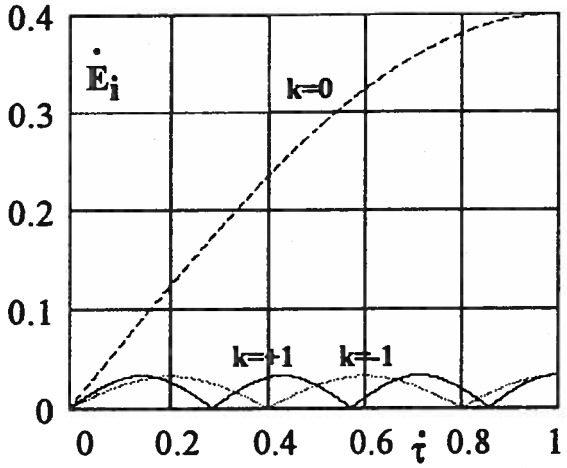

Fig.2 Amplitude of the harmonic e.m.f.s $E_i(k, \dot{I}_i, \dot{\tau})$, generated by the inverse tern currents, for k equal to 0, −1, +1 (e.m.f.s of order 2, 4, 8 referred to the frequency f_s), as a function of $\dot{\tau}$; ($\dot{I}_i$ = 0.1); e.m.f.s expressed in p.u., referred to the quantity $N_t \cdot K_e \cdot f_s \cdot I_n$.

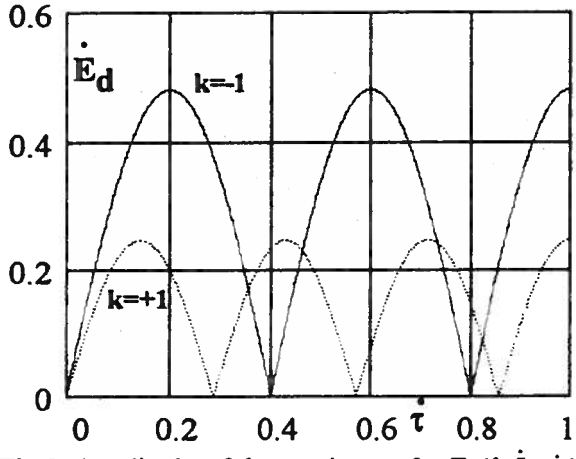

Fig.3 Amplitude of harmonic e.m.f.s $E_d(k, \dot{I}_d, \dot{\tau})$, generated by the direct tern currents, for k equal to −1, +1 (e.m.f.s with order 6 with respect to the frequency f_s), as a function of $\dot{\tau}$; ($\dot{I}_d$ = 1); e.m.f.s expressed in p.u., referred to the quantity $N_t \cdot K_e \cdot f_s \cdot I_n$.

Thus, we can conclude that the presence of the 2nd harmonic e.m.f. induced by the inverse tern is the most important element for detecting the existence of a stator current unbalance, sign of an anomalous operation of the stator guide.

4.3. Choice of the optimal value of the probe winding pitch

The choice of the probe winding pitch must comply with the following requirements:
– the 2nd harmonic e.m.f. signal must be clearly readable by a spectrum analyser, based, for example, on the FFT algorithm: to this aim, the amplitudes of the higher harmonic e.m.f.s must be reduced as much as possible;
– the adopted value of τ must be compatible with the system construction and operating constraints.

In order to guide the choice of the probe winding pitch it is useful to analyse the diagram of the ratios between the lower order e.m.f.s, as a function of $\dot{\tau}$:
– ratios $E_{i(4)}/E_{i(2)}$ and $E_{i(8)}/E_{i(2)}$ between the harmonic e.m.f.s with frequency $4 \cdot f_s$ and $8 \cdot f_s$ and the e.m.f. with f= $2 \cdot f_s$, generated by the inverse tern;
– ratio $E_{dt(6)}/E_{i(2)}$ between the total e.m.f. with f= $6 \cdot f_s$ (sum of the e.m.f.s generated by the 5th and 7th order m.m.f. fields) and the e.m.f. with f= $2 \cdot f_s$.

The diagram of the first couple of ratios is shown in Fig.4, for a value $\dot{I}_i = 0.1$.

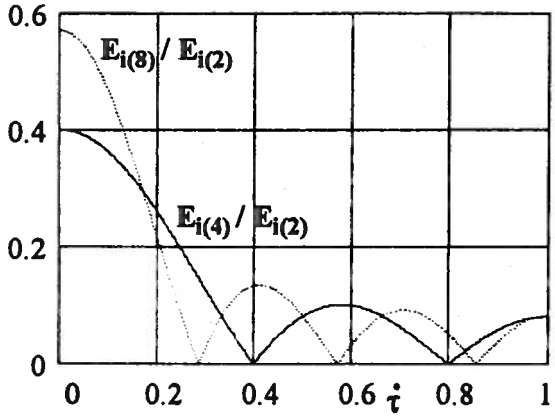

Fig.4 Ratio between the harmonic e.m.f.s with frequency $4 \cdot f_s$ and $8 \cdot f_s$ (due to the harmonic m.m.f.s generated by the currents of the inverse tern) and the harmonic e.m.f. with frequency $2 \cdot f_s$, as a function of the pitch $\dot{\tau}$ of the probe winding ($\dot{I}_i$ = 0.1).

By analysing the Fig.4 we can observe that:
– for every value of the probe winding pitch $\dot{\tau}$, the harmonic e.m.f.s with frequency 8th and 4th are lower than the harmonic e.m.f. with frequency 2nd;
– a value of the pitch that reduces to zero both the higher order harmonics does not exist; thus, for each chosen pitch, one of these harmonics will be always present.

About the direct tern, it has been shown that for each value of k there are two harmonic e.m.f. components with the same frequency: so, they can be added as phasors.

Here the analysis is limited just to the 6th harmonic e.m.f.s (induced by the 5th and 7th order m.m.f.s, produced by the direct tern), because they have the highest amplitude: in order to distinguish the m.m.f. fields that induce these e.m.f.s, in the following they will be indicated as follows: $E_{d[5]}$, $E_{d[7]}$.

With reference to the LSM phasor diagram, called β the angle between the phasors armature current and field current, it has been shown [1] that, while varying β, the e.m.f.s induced in one active conductor are subjected to a phase displacement equal to:

$$\beta_h = \beta \cdot |h| \; ; \qquad (23)$$

therefore, the e.m.f.s $E_{d_{[5]}}$ and $E_{d_{[7]}}$ have a reciprocal phase displacement $\Delta\beta$ given by:

$$\Delta\beta = \pi + \beta_7 - \beta_5 = \pi + 2\cdot\beta \; . \qquad (24)$$

The amplitude of the phasor sum of these e.m.f.s is:

$$E_{d_{(6)}} = \sqrt{E_{d_{[5]}}^2 + E_{d_{[7]}}^2 + 2\cdot E_{d_{[5]}} \cdot E_{d_{[7]}} \cdot \cos(\Delta\beta)} \; . (25)$$

The maximum value ($E_{dt_{(6)}}$) of $E_{d_{(6)}}$ is obtained for $\beta=\pi/2$, occurring when the two phasors are in phase.

Fig.5 shows the diagram of the ratio $E_{dt_{(6)}}/E_{i_{(2)}}$ as a function of the pitch $\dot{\tau}$, for two values of the p.u. inverse current component $\dot{I}_i$.

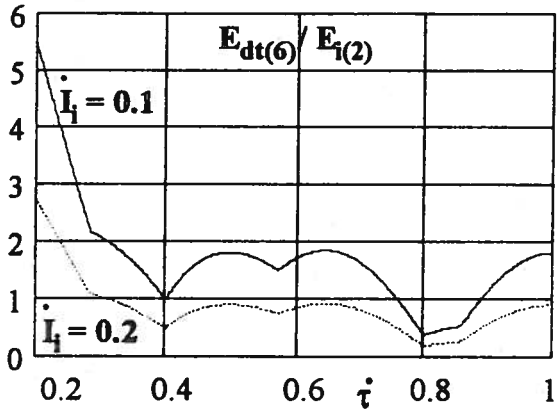

Fig.5 Ratio between the maximum value of the harmonic e.m.f. with $f=6\cdot f_s$ (due to the harmonic m.m.f.s produced by the direct tern currents) and the harmonic e.m.f. with $f=2\cdot f_s$, as a function of the pitch $\dot{\tau}$ of the probe winding ($\dot{I}_i = 0.1 ; 0.2$).

The observation of the Fig.s 4 and 5 suggests that:

- there are various values of τ that reduce the amplitude of the higher harmonic e.m.f.s, thus allowing a good resolution of the $E_{i_{(2)}}$ measurement by FFT;
- in particular, the choice of $\dot{\tau}=0.8$ would lead to make zero the $E_{i_{(4)}}$, at the same time greatly reducing the amplitudes of $E_{i_{(8)}}$ and of $E_{dt_{(6)}}$;
- on the other hand, the choice $\dot{\tau}=0.8$ is not compatible with the constructional constraints: the pole piece (inside which the probe winding must be disposed) is usually extended to roughly $(2/3)\cdot\tau_s$.

Another possible good choice is $\dot{\tau} = 0.4$; in fact:

- this pitch value is perfectly compatible with the construction constraints;
- with this $\dot{\tau}$ value, the 4th order harmonic e.m.f. is zero, while the 8th one has an amplitude reduced to roughly $0.1\cdot E_{i_{(2)}}$;
- for values of the current unbalance corresponding to $\dot{I}_i = 0.1$ the maximum amplitude of the e.m.f. $E_{dt_{(6)}}$ equals the amplitude of $E_{i_{(2)}}$, while the last one is higher for greater unbalance levels;
- on the other hand, for operation conditions with $\beta\neq\pi/2$, the amplitude of $E_{d_{(6)}}$ is even smaller, with additional advantages in the $E_{i_{(2)}}$ measurement.

Therefore, we can conclude that it is possible and convenient to adopt the value $\tau = 0.4\cdot\tau_s$ for the pitch of the probe winding.

4.4. Remarks on the effects of the tooth-slot variation and on the presence of the on-board linear generator

As known, the tooth-slot permeance variation, that occurs during the motion between the pole pieces and the stator structure faced to them, produces an effect of modulation of the field flux: thus, the flux consists of constant and variable overlapped components.

The fundamental frequency of this flux variation is linked to the number of tooth-slot variations occurring during a vehicle displacement equal to a double pole pitch of the stator winding: in the case of q=1, this number of variations equals 6; thus, the fundamental harmonic e.m.f. induced by this effect has frequency $6\cdot f_s$.

This flux variation is detected also by the probe winding and generates an induced e.m.f. with the same frequency, by "transformer effect"; on the other hand, this e.m.f. does not depend on the unbalance level of the armature currents; finally, this e.m.f. composes itself with the 6th frequency e.m.f. induced by the 5th and 7th order harmonic m.m.f.s generated by the direct tern of the stator currents.

In conclusion, the presence of this e.m.f. with $f=6\cdot f_s$ does not affect the $E_{i_{(2)}}$, that represents the sign of the current unbalance, thus constituting the evidence of potential or actual faults.

The amplitude of the e.m.f. due to the "transformer effect" depends, among other things, on the ratio between the probe winding pitch τ and the LSM slot pitch ($\tau_s/3$ for q=1).

Let assume, as a first approximation, that the stator tooth and slot widths are roughly equal: in this case, the following limit situations can occur:

- the maximum amplitude of the e.m.f. with $f=6\cdot f_s$ (due to the tooth-slot permeance variation) occurs for τ equal to a multiple odd of half slot pitch:

$$\tau = (2 \cdot n + 1) \cdot \tau_s / 6 \ , \qquad (26)$$

with n positive integer;

- the minimum amplitude of the e.m.f. with $f=6 \cdot f_s$ (due to the tooth-slot permeance variation) occurs for τ equal to a multiple even of half slot pitch:

$$\tau = (2 \cdot n) \cdot \tau_s / 6 \ . \qquad (27)$$

Of course, the interesting "n" value in (26) and (27) is n=1: as a consequence, the choice $\tau = 0.4 \cdot \tau_s$ (see Fig.6) produces a permeance variation e.m.f. whose amplitude is intermediate among the discussed limits.

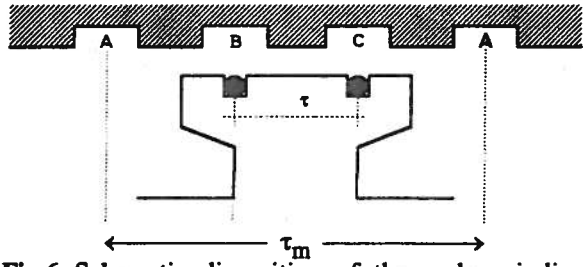

Fig.6 Schematic disposition of the probe winding with pitch $\tau = 0.4 \cdot \tau_s$, disposed in slots obtained along the pole piece of the LSM.

As regards the effect on the probe winding signal of the presence of possible windings of linear synchronous generators (LSG), also disposed in the slots obtained in the pole pieces, the following remarks arise:

- the presence of the slots of the LSG produces an additional contribution to the field flux modulation: moreover, it can be shown that also this effect generates harmonic e.m.f.s with $f=6 \cdot f_s$, thus distinguished by the 2nd harmonic e.m.f.;
- in the loaded operation of the LSG (usually connected to an a.c.-d.c. converter only) the corresponding circulation of currents in the LSG active conductors produces additional m.m.f. contributions at the air gap; nevertheless, their presence does not modify practically the described operation of the probe winding, for the following reasons:
  - the amplitude of the m.m.f.s produced by the loaded operation of the LSG is greatly lower compared with the m.m.f.s generated by the LSM (there is a ratio of roughly $1/10^3$ between the corresponding powers);
  - it can be shown that the main effect of these m.m.f.s is the creation of a further 6th frequency e.m.f., whose amplitude depends on the mutual coupling among LSG and probe winding.

Therefore, while the amplitude of the harmonic e.m.f.s evaluated by means of the previous described model is affected by the "tooth effect", one can conclude that, in any case, the double frequency harmonic e.m.f. is generated in the probe winding only when the armature current unbalance occurs: thus, the probe winding is suited to adequately perform its diagnostic function.

5. Preliminary experimental tests

Some tests have been performed, aiming to obtain first experimental results, using an apparatus composed as described in the following:

- salient-pole rotating synchronous machine, with constant air-gap (main data in Table III);
- probe winding with $\tau = 0.4 \cdot \tau_s$, placed on the air-gap surface of one rotor pole, whose terminals feed a signal transmitter;
- FM signal transmitter (placed on the shaft and battery fed), with an infrared LED transmission;
- signal receiver, fixed on the machine frame, for the conversion of the signal in electrical form;
- 7th order, low pass, active filter, with cut off frequency equal to 1800 Hz;
- 10 bit A/D converter, connected to a PC.

Table III - Main data of the three-phase rotating synchronous machine used for the experimental tests

rated power [kVA]	200
rated voltage [V]	480
rated frequency [Hz]	42
number of poles	6
internal diameter; air-gap [mm]	720; 5

Of course, the transmitter and the receiver (here used for the signal transmission from a rotating to a fixed part of the machine) would not be present in a real Maglev system, equipped with on-board FFT signal processors.

In order to simplify the tests, the synchronous machine has been operated as a generator instead of as a motor; the phase windings have been individually loaded with three star-connected separately adjustable resistors, to obtain the desired unbalance levels of the stator currents.

Some tests have been performed, by varying the stator operating frequency f_s of the machine, the field current, the amplitude and the unbalance level of the armature currents.

As an example, Fig.s 7 and 8 show the amplitude harmonic spectra of the voltages measured at the terminals of the probe winding, in case of balanced and unbalanced currents respectively. More precisely, the shown voltages V_{mh} are the output voltages of the low-pass filter (the corresponding harmonic voltages per turn of the probe winding can be obtained by dividing the V_{mh} by 6.25).

The following should be remarked:

- the Fig.s 7 and 8 (f_s=18 Hz < f_n=42 Hz; I≈20 A « I_n=240 A) have been chosen among the tested operating conditions: in fact, they better show the good behaviour of the probe winding, suited to measure the harmonic voltages both in the balanced and in the unbalanced operation even at low frequency and with weak armature currents;
- if we neglect the existence of a few noise (anyhow characterised by small amplitude), Fig.7 clearly

shows the harmonic voltages produced by the harmonic m.m.f.s generated by the direct tern currents only: in fact, these voltages are induced at the frequencies: 108 Hz=6·f_s; 216 Hz=12·f_s; 324 Hz=18·f_s; 432 Hz=24·f_s;

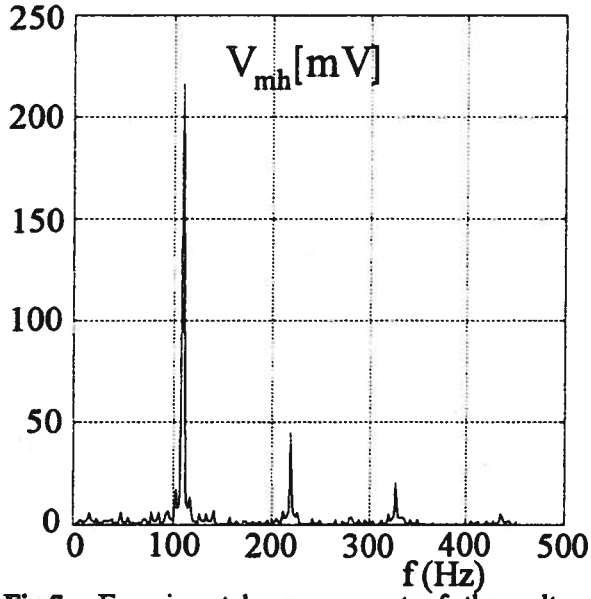

Fig.7 Experimental measurement of the voltage amplitude harmonic spectrum of the probe winding placed on the machine of Table III; operation with balanced stator currents (I_a=I_b=I_c=20.0 A); stator frequency: f_s = 18 Hz.

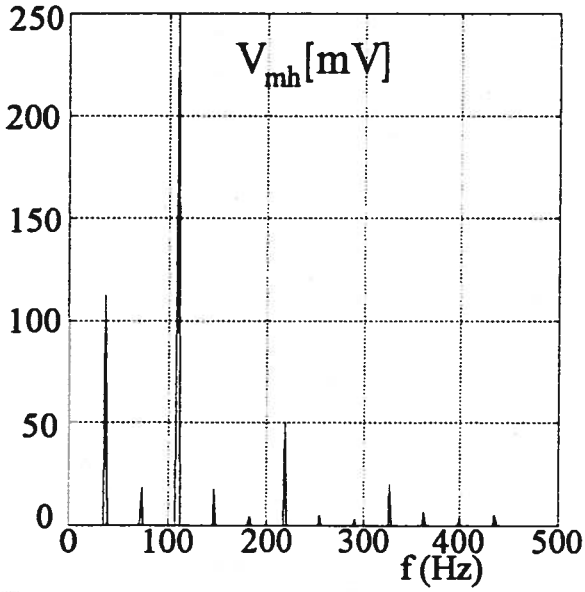

Fig.8 Experimental measurement of the voltage amplitude harmonic spectrum of the probe winding placed on the machine of Table III; operation with unbalanced stator currents (I_a=I_b=20.5 A; I_c=23.5 A; unbalance level ρ_I = 0.096); stator frequency: f_s = 18 Hz.

- Fig.8 shows that, besides the voltages already present in Fig.7, other voltages are induced. These are generated by the harmonic m.m.f.s produced by the inverse tern currents, with the following frequencies: 36 Hz=2·f_s; 72 Hz=4·f_s; 144 Hz=8·f_s; 180 Hz=10·f_s; 252 Hz=14·f_s; 288 Hz=16·f_s; 360 Hz=20·f_s;
- the 4th order harmonic voltage is non zero due to the imperfect construction of the probe winding;
- the harmonic voltages with frequency 6·f_s, 12·f_s, 18·f_s, 24·f_s of Fig.8 have slightly higher amplitudes compared with those of Fig.7, due to the higher amplitude of the stator currents in the second case;
- the 2nd harmonic voltage shows an enhanced amplitude compared with the others, accordingly to what follows from the choice τ= 0.4·τ_s; moreover, it has an amplitude suited to be clearly identified.

In conclusion, these tests confirm the validity of the theoretical analysis.

6. Conclusions

In the present paper the possibility to perform a real time diagnostic monitoring of the operating conditions of the stator guide of an EMS Maglev system has been analysed, by means of a probe winding, disposed in the poles of the vehicle excitation-levitation apparatus, able to detect the stator current unbalance.
The harmonic m.m.f. fields have been considered, produced by the LSM operating currents, by examining the corresponding induced e.m.f.s, both in balanced and in unbalanced conditions.
The conclusion of the analysis, confirmed also by preliminary experimental tests, is that the most important harmonic e.m.f. for the detection of the current unbalance is that with a frequency two times that of the LSM feeding voltage.
Moreover, the choice of a probe winding pitch equal to 0.4 times the LSM pitch implies the best attenuation of the higher harmonic e.m.f.s, with favourable effects for the FFT signal processing.
The studies concerning this subject will continue, in particular according to the following lines:

- more complete modelling of the probe winding operation, in order to evaluate in a quantitative manner the effect of the tooth-slot permeance variation and the correlation between the level of damage in the stator windings, the current unbalance level and the level of the diagnostic signal in the probe winding;
- analysis of probe windings consisting of several coils distributed along the pole pieces and series connected, in order to attenuate further on the higher order harmonic e.m.f.s compared with the double frequency e.m.f., sign of the unbalance;
- further experimental tests, for the systematic analysis of the probe winding operation, when

considering all the variations of the operating and of the construction parameters of the probe winding and of the synchronous machine.

Acknowledgement

The authors warmly thank Dr. G. Esposito, Mr. G. Chiarenza and Mr. A. Bellocchio for the valid help during the realisation of the experimental tests.

References

[1] Di Gerlando, A.; Vistoli, I.: Design Problems of Linear on Board Generators in EMS Maglev Transportation Systems. Maglev'93, 13th International Conference on Magnetically Levitated Systems and Linear Drives. Argonne, Illinois, USA, May 19-21, 1993.

[2] Di Gerlando, A.; Galasso, M; Vistoli, I.: Comparative Analysis of EDS and EMS Maglev Systems. Ibidem.

[3] Ng, J. S.; Harris, A. L.; Amoon, M. E.: Maglev Automated Preventive Maintenance System. Ibidem.

[4] Henning, U.: Present State of Development of Synchronous Long Stator Propulsion System for Transrapid Maglev Trains. Ibidem.

[5] Clessow, G.; Friedrich, R.; Hochbruck, H.; Holzinger, G.: The Long Stator Propulsion System and its Power Supply. Transrapid Maglev System, Hestra Verlag, Darmstadt.

[6] Iwahana, T.; Fujimoto, T.; Maki, N.; Takahashi, H.: A Harmonic Flux Induction Type On-Board Auxiliary Power Source System for Levitated Trains. IEEE Trans. on P.A.S., vol.PAS-100, N°6, June 1981.

[7] Masada, E.; Ohsaki, H.; Tamura, M.; Torii, S.: A Study on the Power Supply for a Superspeed Maglev Transport. IPEC'90.

[8] Sanvito, G.; Sironi, T.: Diagnostics Elements in Trasportation Maglev Systems. Graduation Thesis, Politecnico di Milano (in Italian), 1994.

List of the symbols

B_{M_h} maximum value of the air gap flux density due to the h^{th} harmonic m.m.f. field

e_{d_h} rsm value of the e.m.f. in one active conductor of the probe winding, produced by a h^{th} order m.m.f. of the direct tern of armature currents

e_{i_h} rsm value of the e.m.f. in one active conductor of the probe winding, produced by a h^{th} order m.m.f. of the inverse tern of armature currents

$\dot{e}_{d_h}$ value of e_{d_h}, referred to the product $K_e \cdot f_s \cdot I_n$

$\dot{e}_{i_h}$ value of e_{ih}, referred to the product $K_e \cdot f_s \cdot I_n$

E_d e.m.f. in the probe winding due to the currents of the direct tern

E_i e.m.f. in the probe winding due to the currents of the inverse tern

$E_{d_{[h]}}$ e.m.f. with $f=6 \cdot f_s$, produced by a m.m.f. with order h= 5, 7 (direct tern currents)

$E_{i_{(2)}}$ e.m.f. with $f=2 \cdot f_s$, produced by a fundamental m.m.f. (inverse tern currents)

$E_{i_{(m)}}$ e.m.f. with $f=m \cdot f_s$ (m=4, 8), produced by a m.m.f. with order 5, 7 (inverse tern currents)

f_s feeding frequency of the LSM

f_h frequency of the h^{th} harmonic e.m.f. induced in the probe winding

h harmonic order of the m.m.f.s (h=1+6·k), with k= ±1, ±2, ±3, ...

K_e coefficient: $K_e = (6 \cdot \mu_o \cdot \tau_s \cdot \ell_e)/(\pi \cdot \delta)$

k_{wh} winding factor at the h^{th} harmonic

I rms value of the stator phase current

I_d direct tern component of the armature currents

I_i inverse tern component of the armature currents

$\dot{I}_d$ ratio I_d/I_n

$\dot{I}_i$ ratio I_i/I_d

I_n rated current of the LSM

ℓ_e transversal width of the lamination stack of the LSM (one side)

M_{M_h} amplitude of the h^{th} order m.m.f.

N_t number of turns of the probe winding

q number of stator slots/(pole·phase)

u number of conductors in each stator slot

v_h speed of the h^{th} order m.m.f. field with respect to the vehicle

v_s speed of the fundamental m.m.f. field with respect to the stator

v_{s_h} speed of the h^{th} order m.m.f. field with respect to the stator

V_{mh} harmonic voltage of the probe winding measured at the output terminals of the low-pass filter

α_d e.m.f. in each conductor, referred to the product $K_e \cdot I_d \cdot f_s$

α_i e.m.f. in each conductor, referred to $K_e \cdot I_i \cdot f_s$

β angle between the phasors armature current and field current of the LSM

β_h phase angle of the e.m.f. $E_{d_{[h]}}$ (h=5, 7)

δ air gap width of the LSM

$\Delta\beta$ phase displacement between the e.m.f.s $E_{d_{[5]}}$ and $E_{d_{[7]}}$

τ probe winding pitch

$\dot{\tau}$ ratio τ/τ_s

τ_s pitch of the LSM

τ_{s_h} pitch of the h^{th} harmonic m.m.f. produced by the stator currents

ρ_I unbalance level of the LSM armature currents